

CHAPTER FOUR

PERFORMANCE OF DYE-DOPED PMMA LASERS

4.1 Preliminary experiments

The PMMA slabs (doped with R640 (ClO<sub>4</sub>), R6G (ClO<sub>4</sub>), R6G (Cl), PM546, C460) were excited by using a TE nitrogen laser operating at 1 mJ pulse. The wavelengths and efficiencies of the emitted lasers are tabulated in table 4.1 and four laser spectra are presented in figures 4.1 - 4.4. For comparison purposes, the laser efficiency of the analogous liquid dye laser was measured. Of the dyes studied, R640 and R6G (ClO<sub>4</sub>) were found to be exceptionally efficient, and their optimum concentrations were determined and then used in the subsequent measurements.

Table 4.1 Peak laser wavelength and laser efficiency

| Dye                      | Concentration<br>( $\times 10^{-3}$ M) | Solvent<br>Composition*          | Laser<br>wavelength<br>(nm)<br>in PMMA | Laser<br>efficiency<br>(%)<br>in PMMA | Laser<br>efficiency<br>(%)<br>in liquid |
|--------------------------|--|----------------------------------|--|---------------------------------------|---|
| R6G (ClO <sub>4</sub> )  | 5                                      | 95/5 v/v chloroform/<br>methanol | 582                                    | $8.0 \pm 0.2$                         | $19 \pm 4$                              |
| R6G (Cl)                 | 5                                      | 95/5 v/v chloroform/<br>methanol | 599                                    | <1                                    | <1                                      |
| R640 (ClO <sub>4</sub> ) | 5                                      | Chloroform                       | 660                                    | $7.8 \pm 0.3$                         | $13 \pm 2$                              |
| C460                     | 25                                     | Chloroform                       | 428                                    | $1.7 \pm 0.1$                         | $10 \pm 2$                              |
| PM546                    | 5                                      | Chloroform                       | 538                                    | <1                                    | <1                                      |

\* Solvent composition used in fabrication.

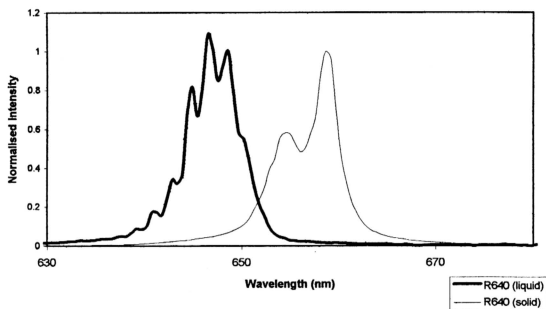


Figure 4.1 Laser spectra of solid-state and liquid dye laser for dye R640 ( $\text{ClO}_4$ )

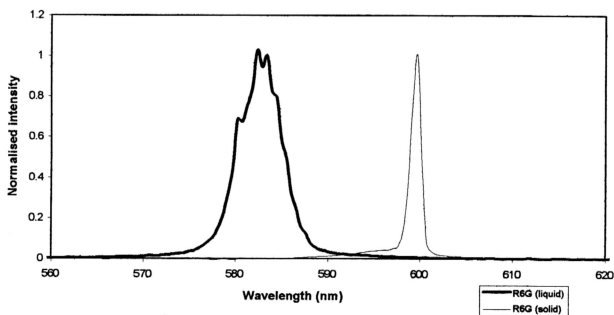


Figure 4.2 Laser spectra of solid-state and liquid dye laser for dye R6G ( $\text{ClO}_4$ )

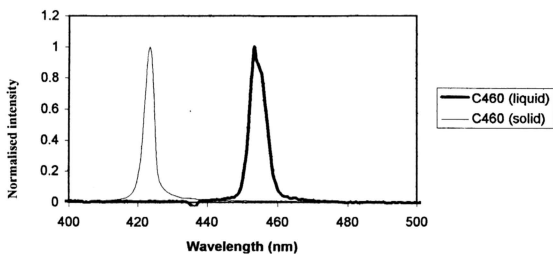


Figure 4.3 Laser spectra of solid-state and liquid dye laser for dye C460

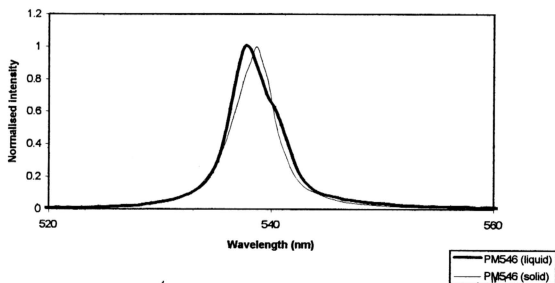


Figure 4.4 Laser spectra of solid-state and liquid dye laser for dye PM546

An inspection of table 4.1 shows that the laser efficiencies of the solid-state dye lasers are lower than those of liquid dye lasers, which can be partly attributed to a higher degree of laser scattering because the solid-state matrix is not homogenous. Another contributing cause can possibly arise from the aggregation of the dye<sup>38</sup>, an explanation that has been invoked in a study of the lasing characteristics of R6G in modified PMMA. Figures 4.1 and 4.2 show that the peak laser wavelength for solid-state R640- and R6G(ClO<sub>4</sub>)<sup>-</sup>-doped PMMA as compared with the liquid systems has been shifted to the red.

Figure 4.3 shows that the C460 dye is shifted by about 30 nm to the blue. As suggested<sup>59</sup>, the magnitude of this shift probably results from the formation of dye aggregates in the PMMA matrix, a shift that is related to the blue shift in the fluorescence spectrum. PM546, decomposed during moulding and no conclusion about the shift could be advanced.

## 4.2 Effect of dye concentration, pumping energy and pumping power on laser efficiency

The laser efficiency is defined as the ratio of the solid-state dye laser output energy to the pumping energy. For those dye-doped PMMA slabs, the dependence of the laser efficiency on the R640 ( $\text{ClO}_4$ ) and R6G ( $\text{ClO}_4$ ) concentrations is shown in figures 4.5 and 4.6. In figure 4.5, a single R640-doped PMMA slab was used for each dye concentration and the highest laser efficiency was found at  $5 \times 10^{-3}$  M. The initial increase of laser efficiency can be ascribed to an increase of resonance radiation trapping that effectively increases the upper laser level lifetime<sup>61</sup>. When the concentration exceeds the optimum value, quenching of the excited dye molecules by ground-state dye molecules (self re-absorption) and the formation of less fluorescent higher-order dye aggregates decreases the efficiency.

The plot of laser efficiency for R6G ( $\text{ClO}_4$ ) (figure 4.6) shows slightly different behaviour. The laser efficiency increases rapidly from about 4 to 8% in the  $5$  to  $10 \times 10^{-4}$  M range. To probe the rapid increase, the laser efficiency was measured without the use of a back mirror: at  $0.5 \times 10^{-3}$  to  $1 \times 10^{-3}$  M, a 50% reduction was found when the back mirror was not used, which implicates the existence of laser oscillations in addition to super-radiant emissions. In contrast, no reduction was observed at higher concentrations (0% at  $7.5 \times 10^{-3}$  M).

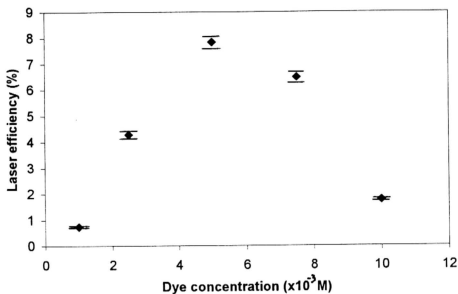


Figure 4.5 Laser efficiency versus dye concentration for R640 (ClO<sub>4</sub>)

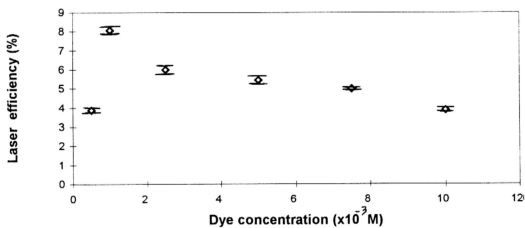


Figure 4.6 Laser efficiency versus dye concentration for R6G (ClO<sub>4</sub>)

The absence suggests that oscillations between the back mirror and the PMMA-air interface were suppressed by the unexcited dye, so that the resulting laser essentially consisted of only super-radiant emissions.

Figure 4.7 shows that the laser efficiency increases with pumping energy for R640 ( $\text{ClO}_4$ )-doped PMMA in the  $2.5 \times 10^{-3}$  -  $1.0 \times 10^{-2}$  M range. The plot shows saturation when the concentration is lowest. The optimum concentration shifts to a higher value on raising the pumping power, as suggested by examining the laser efficiencies when pumped by the 350 kW TE and 75 kW TEA  $\text{N}_2$  laser systems, both operating at 350  $\mu\text{J}$  (figure 4.8). Shorter pulse-width pumping also improves the optimum laser efficiency by about 20%. The pumping energy threshold was reached much earlier when using shorter pumping pulses as an earlier attainment of the energy limit tends to reduce energy losses through other non-radiative processes.

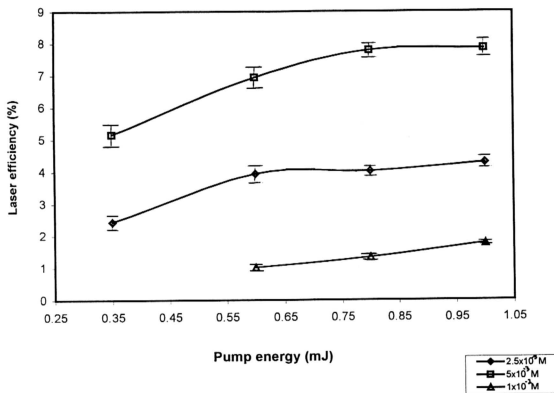
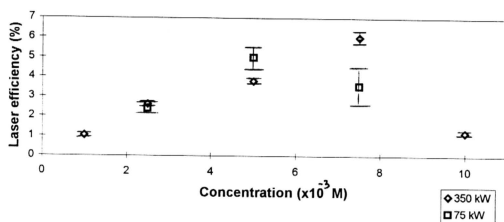


Figure 4.7 Laser efficiency versus pumping energy for R640 ( $\text{ClO}_4$ )





**Figure 4.8** Laser efficiency versus dye concentration are different pumping power for R640 ( $\text{ClO}_4$ )

### 4.3 Effect of dye concentration on the peak laser wavelength

The probability of the absorption and re-emission of a laser photon is expected to increase with increasing dye concentration. However, since part of the absorbed photon-energy is lost as vibrational and rotational energies, the re-emitted photon must be of a higher wavelength than of the absorbed photon. The peak laser wavelengths of R6G ( $\text{ClO}_4$ )-doped PMMA slabs showed an increase with increasing dye concentration in the  $5 \times 10^{-4}$  -  $2.5 \times 10^{-3}$  M range to a maximum of 599 nm (figure 4.9).

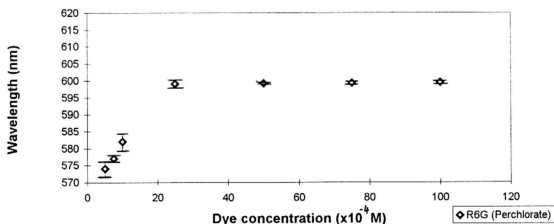


Figure 4.9 Peak laser wavelength versus dye concentration for R6G ( $\text{ClO}_4$ )

## 4.4 Photo bleaching

The dye laser efficiency for R640- and R6G ( $\text{ClO}_4$ )-doped PMMA as probed by measuring the laser output when the TE  $\text{N}_2$  laser beam was focussed on to a fixed position of the slab was found to drop gradually as a function of the number of pulses (figure 4.10). The drop in the laser efficiency has been attributed to photo-degradation of the dyes, as can be observed in a study on the laser efficiency of R6G in modified PMMA<sup>18, 38</sup>. Dye photo-stability has been reported<sup>12</sup> to be improved by the incorporation of low molecular-weight additives in PMMA that retard the formation of free radicals through resonance vibration cross-relaxation for Xanthene dyes. When excited to the singlet  $S_n$  ( $n > 1$ ) state, the dye transfers its energy to the surrounding polymer chains. These polymer chains dissipate the energy through vibrational processes, which may break up the chains to form free radicals<sup>18, 41</sup>.

R6G ( $\text{ClO}_4$ ), which belongs to the Xanthene family, is about thirteen times more stable than R640 ( $\text{ClO}_4$ ) (figure 4.10) under the same pumping conditions.

Photo bleaching is not expected to occur during the earlier stages of pumping, so that the initial differences in laser efficiencies must necessarily arise from thermal factors only. As shown in the laser efficiency-pump pulses plot (figure 4.11), the initial laser efficiency (i.e., number of pump pulses = 0), is

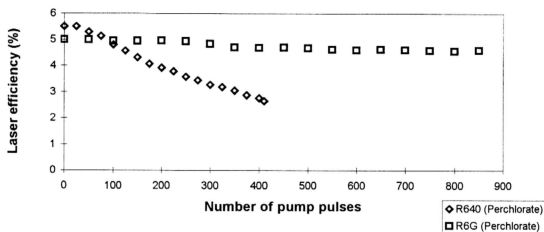


Figure 4.10 Laser efficiency versus number of pumping for R640 ( $\text{ClO}_4$ ) and R6G ( $\text{ClO}_4$ )

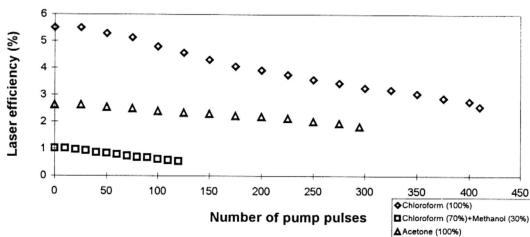


Figure 4.11 Laser efficiency versus number of pumping for R640 ( $\text{ClO}_4$ ) for different solvent systems

largest when 100% chloroform was used in the fabrication of the preform. For the three solvent systems, the laser efficiencies of the ultimate solid-state dye lasers decrease with increasing pulses (table 4.2). The rate of decrease is largest for the 70/30 chloroform/methanol mixture. Clearly, the manifestation of such differences must arise from the presence of solvent molecules trapped in the PMMA slab, but this was not further investigated. Indeed, a study on the residual solvent in PMMA film with quadrupole mass spectroscopy<sup>56</sup> has confirmed the existence of solvent molecules in PMMA despite the sample being dried in vacuum for several hours.

Table 4.2 Drop in laser efficiency per pumping

| Solvent                       | Drop in laser efficiency per pumping pulse |
|-------------------------------|--|
| chloroform                    | -0.13                                      |
| acetone                       | -0.12                                      |
| 70/30 v/v chloroform/methanol | -0.39                                      |

Pumped by long pulse TE N<sub>2</sub> laser with pulse energy  $\approx 1$  mJ

## 4.5 Thermal degradation of dyes during fabrication

The thermal degradation of dyes during fabrication was studied by varying first the dye, and then the solvent system used to dissolve the PMMA-dye mixture for the preform. The degree of thermal degradation was estimated from the area-under-the-curve in the fluorescence and absorption spectra. The control consisted of an identical concentration of dye in pure chloroform. The results are tabulated in table 4.3 and illustrated in figures 4.12 and 4.13; for comparison purposes, the corresponding laser efficiencies are also included in the table.

Large losses in fluorescence (90%) and absorption (80%) intensities for R6G ( $\text{Cl}$ ) confirm that most of the dye had degraded in the fabrication. Curiously, R6G ( $\text{ClO}_4$ ), which has the identical coumarin-based cation, R640 ( $\text{ClO}_4$ ) and C460 showed no degradation, unlike PM546, which lost more than half its fluorescence.

The nature of the solvent systems show a similar effect on thermal decomposition, non-polar chloroform showing the highest fluorescence intensity and the polar 70/30 chloroform/methanol mixture the lowest (figure 4.14). The most fluorescent solvent system resulted in the highest laser efficiency (table 4.4).

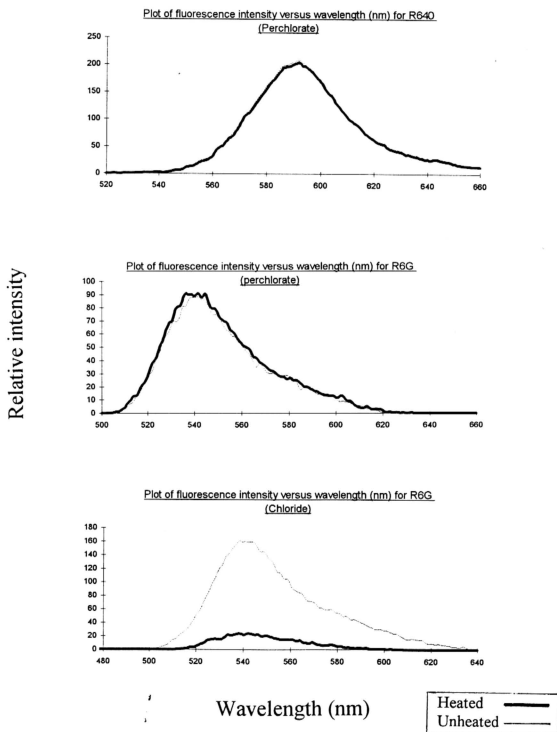


Figure 4.12 Fluorescence spectra of dyes after fabrication as compare with the control (part 1)

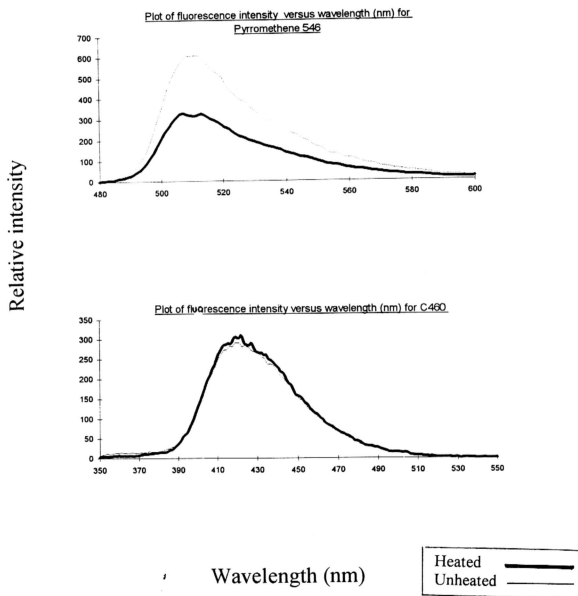
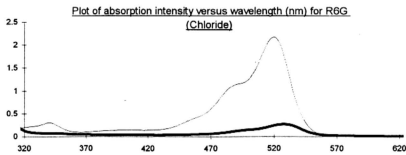
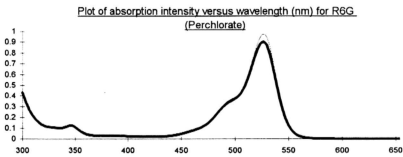
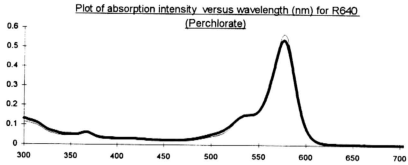


Figure 4.12 Fluorescence spectra of dyes after fabrication as compare with the control (part 2)



Relative intensity



Wavelength (nm)

|          |       |
|----------|-------|
| Heated   | —     |
| Unheated | - - - |

Figure 4.13 Absorption spectra of dyes after fabrication as compare with the control (part 1)

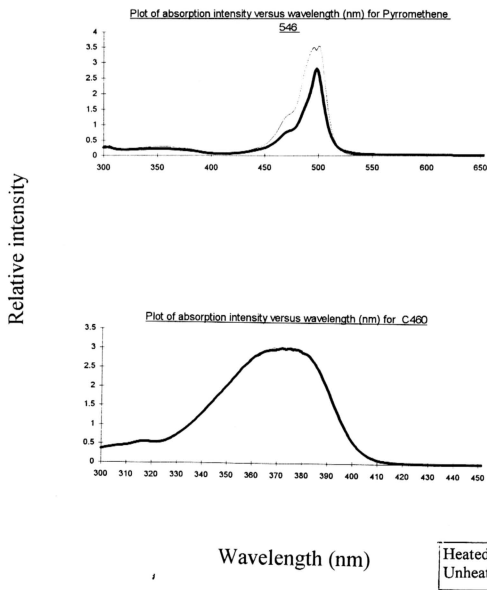
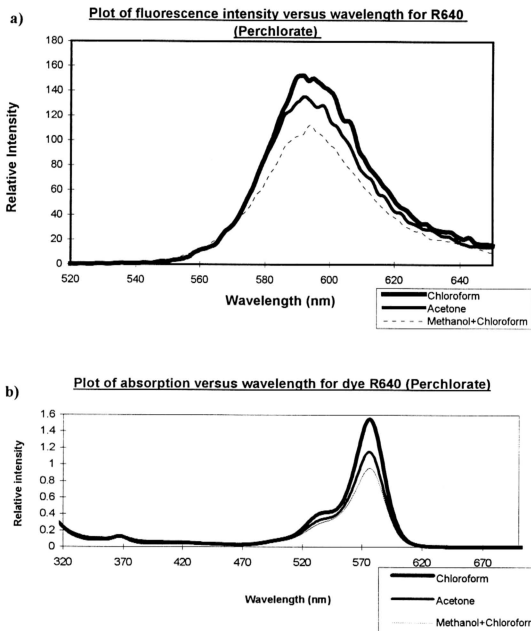


Figure 4.13 Absorption spectra of dyes after fabrication as compare with the control (part 2)



**Figure 4.14** a) Fluorescence spectra of R640 for different solvent systems  
b) Absorption spectra of R640 for different solvent systems

Table 4.3 Drop in fluorescence and absorption intensities, and the corresponding laser efficiencies

| Type of dye              | Change of fluorescence intensity (%) | Change of absorption intensity (%) | Laser efficiency (%) |
|--------------------------|--------------------------------------|------------------------------------|----------------------|
| R6G (ClO <sub>4</sub> )  | 0                                    | 0                                  | 8                    |
| R6G (Cl)                 | -88                                  | -79                                | <1                   |
| R640 (ClO <sub>4</sub> ) | 0                                    | 0                                  | 7.8                  |
| C460                     | 0                                    | 0                                  | 1.7                  |
| PM546                    | -44                                  | -29                                | <1                   |

Table 4.4 Laser efficiency

| Solvent                   | Laser efficiency |
|---------------------------|------------------|
| chloroform                | 5.5%             |
| acetone                   | 2.6%             |
| 70/30 chloroform/methanol | 1.0%             |

Pumped by a long pulse TE N<sub>2</sub> laser operating at 1 mJ pulse.

## 4.6 Summary

A hot-press moulding method was used for the fabrication of R640 ( $\text{ClO}_4$ )- and R6G ( $\text{ClO}_4$ )-impregnated poly(methylmethacrylate) (PMMA) dye lasers. The dyes were incorporated into the PMMA matrix by dissolving both the dye and PMMA in an organic solvent; evaporation of the solvent in a  $175^\circ\text{C}$  vacuum oven furnished a spongy material, which was then moulded into solid-state dye lasers of approximately 8% efficiency. R6G ( $\text{ClO}_4$ )-doped PMMA slabs suffered only a <10% drop in efficiency after having been operated for 850 pulses at 0.3 Hz. Moulding the preform at <1 mbar eliminated the formation of air bubbles in the slabs, and annealing the slabs minimised light scattering caused by the presence of adventitious solvent trapped in the matrix. The thermal stability of the dyes and the operational lifetime of the dye lasers depended on the nature of the solvent system that was used in the preparation of the preform. This study documents the first example of the use of a hot-press moulding procedure for solid-state dye lasers that completely eliminates the radical-initiated decomposition of dyes, a problem associated with conventional fabrication methods in which the monomers are polymerised in the presence of the dyes.